

# TPR is a prognostic biomarker and potential therapeutic target associated with immune infiltration in hepatocellular carcinoma

TENG LONG<sup>1,2\*</sup>, WEIJIE WU<sup>1,2\*</sup>, XIN WANG<sup>1,2</sup> and MINSHAN CHEN<sup>1,2</sup>

<sup>1</sup>State Key Laboratory of Oncology in South China and <sup>2</sup>Department of Liver Surgery, Sun Yat-sen University Cancer Center, Guangzhou, Guangdong 510060, P.R. China

Received January 9, 2023; Accepted June 14, 2023

DOI: 10.3892/mco.2024.2725

**Abstract.** Liver cancer is the fourth leading cause of cancer-related mortality worldwide and hepatocellular carcinoma (HCC) is the most common primary liver cancer. In the present study, it was demonstrated that translocated promoter region (TPR) was upregulated in tumor tissues and associated with prognosis and immune infiltration in HCC. The clinical outcome of patients with HCC with aberrant expression of TPR was examined using multiple databases, including Gene Expression Omnibus, The Cancer Genome Atlas (TCGA), Genotype-Tissue Expression, Kaplan-Meier (KM) Plotter and Xiantao tool. The clinicopathologic characteristics of patients from TCGA database that were associated with overall survival were assessed using Cox regression and KM analysis. The potential hallmarks associated with TPR expression were further predicted by Metascape and Gene Set Enrichment Analysis, and the relationship between TPR and immune infiltration was explored using the Tumor-Immune System Interactions Database and the Tumor Immune Estimation Resource. The results demonstrated that TPR expression was higher in HCC and its overexpression was associated with a worse prognosis, alongside a correlation with several clinical features. Furthermore, cell differentiation, a prospective new hallmark of cancer, was differentially enriched in the high TPR expression phenotype pathway. Moreover, TPR may also modulate the tumor immune microenvironment as it was significantly associated with immunoregulators and chemokines, as well as different tumor infiltration immune cells. According to the *in vitro* experiments, TPR silencing inhibited

the phosphorylation of AKT and the proliferation of HCC cells. In summary, TPR may be a new marker and target for HCC therapy.

## Introduction

Liver cancer is the sixth most commonly diagnosed cancer and the third leading cause of cancer-related mortality worldwide (1). Hepatocellular carcinoma (HCC) is the most common primary liver cancer and accounts for 75-85% of cases (2). Currently, the potentially curative treatments for HCC are ablation, surgical resection and transplantation (3). Despite the advances in chemotherapy, radiotherapy, immunotherapy and liver transplantation, HCC prognosis remains poor due to the high risk of recurrence and metastases (4). The highly heterogeneous nature of HCC leads to difficulties in diagnosing or predicting disease using existing biomarkers (5). Therefore, it is urgent to identify novel driver genes for HCC treatment, which will improve the survival of patients with HCC.

Translocated promoter region (TPR) is a coiled-coil homodimer and has a rod-like shape (6-8). TPR consists of two domains: An N-terminal domain consisting of ~1,600 amino acids that forms a parallel two-stranded coil and is interrupted periodically throughout its length, and a C-terminal domain that features 800 non-helical amino acids enriched in acidic residues (8-11). As with numerous transcription-regulating nucleoporins (NUPs), TPR is localized to the nucleus (12). In addition, TPR binds chromatin *in vitro* and is essential for the formation of heterochromatin exclusion zones near nuclear pore complexes (13,14). TPR plays a number of roles in the nucleus, including regulating the three prime repair exonuclease 2-dependent mRNA export pathway (15,16) and scaffolding ERK2 (17) and MYC (18) enzymes. Several studies have demonstrated that TPR is implicated in multiple types of cancers, including lung adenocarcinoma (19,20), ependymoma (21), glioma (22) and colon cancer (23). However, little research has been conducted on HCC. Therefore, the purpose of the present study was to discover the potential mechanisms by which TPR may contribute to tumorigenesis and immune involvement in HCC.

The development of numerous database platforms has led to significant advances in cancer bioinformatics research, which allows researchers to screen markers for cancer more easily. Thus, in the present study, TPR was identified as a significantly

---

*Correspondence to:* Professor Minshan Chen or Professor Xin Wang, State Key Laboratory of Oncology in South China, Sun Yat-sen University Cancer Center, 651 Dongfeng East Road, Guangzhou, Guangdong 510060, P.R. China  
E-mail: chenmsh@sysucc.org.cn  
E-mail: wangxin1@sysucc.org.cn

\*Contributed equally

**Key words:** translocated promoter region, hepatocellular carcinoma, marker, prognosis, immune checkpoints

upregulated gene in HCC using the Gene Expression Omnibus (GEO). To clarify the biological functions of TPR in HCC, Xiantao tool, The Cancer Genome Atlas (TCGA), the Genotype-Tissue Expression (GTEx) and the Kaplan-Meier (KM) Plotter were used to determine whether the expression of TPR was related to the clinical outcome of HCC. Next, gene-set enrichment of TPR was conducted using the Metascape database and Xiantao tool. In addition, investigation of TPR and immune cell infiltration was performed using Xiantao tool and the Tumor Immune Estimation Resource (TIMER) database. Finally, analyses of immune-modulators and chemokines were further conducted using data from the Tumor-Immune System Interactions Database (TISIDB). In the present study, TPR was identified as being important in HCC, and it was indicated that TPR may be involved in promoting tumor progression in cells.

## Materials and methods

**Patient datasets.** The gene expression profile data (GSE36376, GSE39791 and GSE60502) were downloaded from the GEO (<http://www.ncbi.nlm.nih.gov/geo/geo2r>) (24–26). The inclusion criteria for genomics data were as follow: i) The samples were obtained from *Homo sapiens*; ii) all tissues were classified as HCC or normal tissues; and iii) the sample sizes were >10 per study. GSE36376 included 240 HCC tumor tissues and 193 adjacent non-tumor tissues; GSE39791 included 72 tumor tissues and 72 matched adjacent non-tumor tissues; GSE60502 included 18 tumor tissues and 18 adjacent non-tumor tissues. GEO2R (<http://www.ncbi.nlm.nih.gov/geo/geo2r>) was used to analyze differentially expressed genes (DEGs) between HCC and non-tumor samples. The cut-off was set as  $\log_2$  fold change (FC)>1 and adjusted  $P<0.01$ . TPR expression and clinical data were obtained from TCGA (<https://portal.gdc.cancer.gov/>) and GTEx (<https://gtexportal.org/home/>). Given that the data were obtained from the online databases, additional approval from an ethics committee was not required.

**Analysis of TPR expression in tumor and normal tissues.** Xiantao tool (<https://www.xiantao.love/>) is a platform using R software (3.6.3) for acquiring data from TCGA and GTEx. TPR expression in HCC tissues, tissues adjacent to carcinoma and normal tissues was compared using Xiantao tool and presented in box, scatter and violin plots. Diagnostic performance of TPR was assessed using receiver-operating characteristic curves performed on Xiantao tool. All the DEGs ( $\log_2$ FC>1.5 and adjusted  $P<0.05$ ) gained from single gene differential analysis through Xiantao tool were presented in volcano plots.

**Humantissue specimens.** A total of 14 pairs of HCC and matched normal fresh frozen tissues were obtained through hepatectomy at Sun Yat-sen University Cancer Center (Guangzhou, China), from 2019 to 2021 (12 males and 2 females, ages from 20 to 78 years with an average age of 56). The patients were diagnosed according to their clinicopathologic characteristics at the Sun Yat-sen University Cancer Center. No patients had received radiotherapy and/or chemotherapy prior to surgery. Informed consent was obtained from all patients and approved (approval no. B2022-238-02) by the Research Medical Ethics Committee of Sun Yat-sen University Cancer Center.

**Cell culture.** The liver cancer cell lines (Hep3B, SNU449, MHCC97H, Huh7, HepG2 and HCCLM3) were obtained from the American Type Culture Collection (ATCC) and cultured according to the instructions from the ATCC. All cells were grown in DMEM supplemented with 10% FBS (both from Invitrogen; Thermo Fisher Scientific, Inc.) at 37°C and 5% CO<sub>2</sub>. All cell lines in the present study were authenticated utilizing short-tandem repeat profiling.

**RNA extraction and reverse transcription-quantitative PCR (RT-qPCR).** The total RNA of the liver cancer cell lines (Hep3B, SNU449, MHCC97H, Huh7, HepG2 and HCCLM3) or tissue was isolated utilizing TRIzol® reagent (Invitrogen; Thermo Fisher Scientific, Inc.) according to the manufacturer's instructions. First-strand cDNA was synthesized utilizing the Revert Aid™ First Strand cDNA Synthesis Kit (Fermentas; Thermo Fisher Scientific, Inc.). The thermocycling conditions used were as follows: 37°C for 15 min, 95°C for 5 sec and were then cooled to 4°C upon completion. Quantitative PCR assays were performed using a A28134 QuantStudio® 5 Real-Time PCR Instrument (Thermo Fisher Scientific, Inc.) and iTaq Universal SYBR Green Supermix reagent (Bio-Rad Laboratories, Inc.). The thermocycling conditions used were as follows: 95°C for 30 sec, 40 cycles at 95°C for 3 sec and 60°C for 30 sec, then 60°C for 20 sec and 95°C for 1 sec. The relative expression of each gene was calculated using the  $2^{-\Delta\Delta C_q}$  method with GAPDH as the internal reference (27). The primers used to amplify the indicated genes are shown in Table SI.

**Interaction network analysis.** The GeneMANIA database (<http://www.genemania.org>) was used to explore the genes that interacted with TPR. The Search Tool for Interaction Gene/Proteins (STITCH) website (<http://stitch.embl.de/>) was used to analyze the protein-protein interactions of TPR.

**Tumor immune infiltration analysis.** TIMER (<https://cistrome.shinyapps.io/timer/>) and Xiantao tool were used to analyze the infiltration levels of different immune cells. TIMER was also applied to explore the interrelation between TPR expression and different gene marker sets of immune cells. The correlations were evaluated by purity-correlated partial Spearman's correlation. An integrated repository portal for TISIDB (<http://cis.hku.hk/TISIDB/>) was used to investigate the relationship between TPR and immunoinhibitors, immunostimulators, chemokines and receptors.

**Enrichment analysis.** Metascape (<http://metascape.org/>) and Xiantao tool was used to perform Gene Ontology (GO) and Kyoto Encyclopedia of Genes and Genomes (KEGG) analysis to explore the biological processes (BPs), cellular components (CCs) and molecular functions (MFs) of TPR in HCC. Gene Set Enrichment Analysis (GSEA) was used to probe the potential mechanisms of TPR performed on Xiantao tool. Gene sets with false discovery rate (FDR) <0.25 and  $P$  adjust <0.05 were considered as significant.

**Small interfering RNA (siRNA) treatment.** The oligonucleotide sequences targeting TPR mRNA were as follows: #1, GCAGCTTGTTGATTCCATA (5'-3') and #2, GGAGCGATCTGAAACAGAA (5'-3') synthesized from Guangzhou RiboBio Co., Ltd.

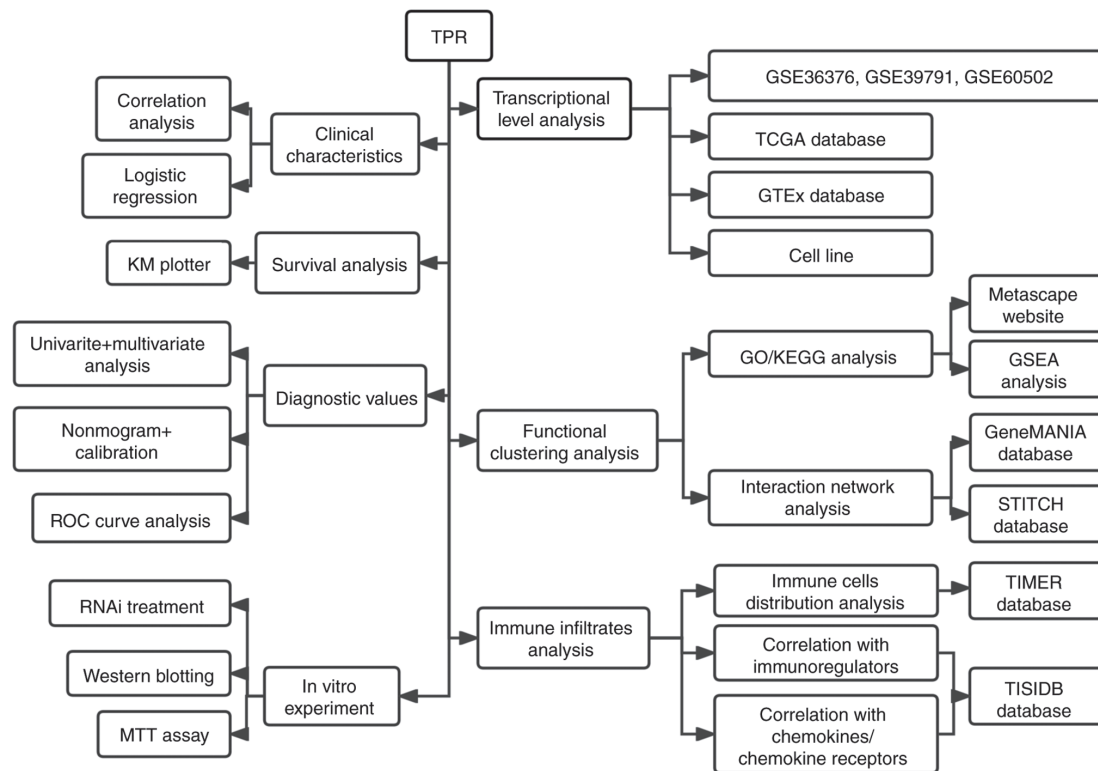


Figure 1. Flow diagram of the databases and methods used in the present study.

The siRNA negative control (siN0000001-1-5) is designed and produced by Guangzhou RiboBio Co., Ltd. and its sequence is proprietary (28). Transfection was performed according to the manufacturer's instructions using Lipofectamine RNAi MAX transfection reagent (Invitrogen; Thermo Fisher Scientific, Inc.) and 50 nM siRNA. siRNA transfection was performed at 37°C for 6 h and the culture medium was then replaced with fresh culture medium. Follow-up procedures were performed 24 h later.

**Western blotting (WB).** Briefly, the liver cancer cell lines Hep3B and SNU449 were collected, lysed in RIPA buffer (150 mM NaCl, 0.5% EDTA, 50 mM Tris, 0.5% NP40, pH=8.0) and centrifuged for 20 min at 13,500 x g and 4°C. The protein concentration was measured using a BCA Protein Assay Kit (Beijing Solarbio Science & Technology Co., Ltd.). The proteins (20 µg/lane) were separated using SDS-PAGE electrophoresis in 4 to 20% polyacrylamide gels and transferred to PVDF membranes (Invitrogen; Thermo Fisher Scientific, Inc.). The PVDF containing protein membranes were blocked in 5% skim milk at room temperature for 120 min. The membranes were then incubated overnight with primary antibodies against AKT (1:1,000), phosphorylated (p)-AKT (1:1,000) or GAPDH (1:1,000) at 4°C. Membranes were then washed with TBST with 0.1% Tween-20 and incubated with goat anti-rabbit IgG (H&L) HRP secondary antibodies (1:10,000) at 25°C for 1 h. The protein bands were then visualized using the ECL chemiluminescence system (Pierce; Thermo Fisher Scientific, Inc.). The antibodies used in the present study are shown in Table SII.

**3-(4,5-dimethylthiazol-2-yl)-2,5-diphenyltetrazolium bromide (MTT) assay.** An MTT assay was conducted to measure cell viability. Briefly, SNU449 or Hep3B cells were seeded at a

density of 2,000 cells per well in a 96-well microplate. The cells were incubated with MTT at 37°C for 4 h, then the culture medium was removed, and 200 µl dimethylsulfoxide (DMSO) was added to dissolve the purple formazan. The optical density (OD) was detected at 490 nm with the microplate reader once per day for 5 days. The results are presented as the mean ± SD of three independent experiments.

**Statistical analysis.** Data were collected from three independent experiments. The GraphPad Prism 9 (GraphPad Software; Dotmatics) and the SPSS software (version 16.0, SPSS Inc.) were used for data analysis. Data were presented as the mean ± SD. Unpaired Student's t-test was used to analyze differences between groups and one-way analysis of variance with Tukey's post hoc test was used to analyze multiple groups. Survival analysis was performed using the KM method, and differences among the survival curves were analyzed with the log-rank test. The follow-up threshold was 30 months. Wilcoxon rank sum test was used to analyze  $\alpha$ -fetoprotein (AFP). Dunn's test was used to analyze the pathological stage. Two-way ANOVA with Dunnett's multiple comparison test was used to analyze the MTT assays. P<0.05 was considered to indicate a statistically significant difference.

## Results

**High expression of TPR in HCC and pan-cancer.** The flow diagram presented in Fig. 1 was constructed to reveal the process of the present study. To identify the key genes in the progression of HCC, GSE36376, GSE39791 and GSE60502 datasets were analyzed to explore the DEGs in HCC. As demonstrated by Venn diagram (Fig. 2A), 187 congruous



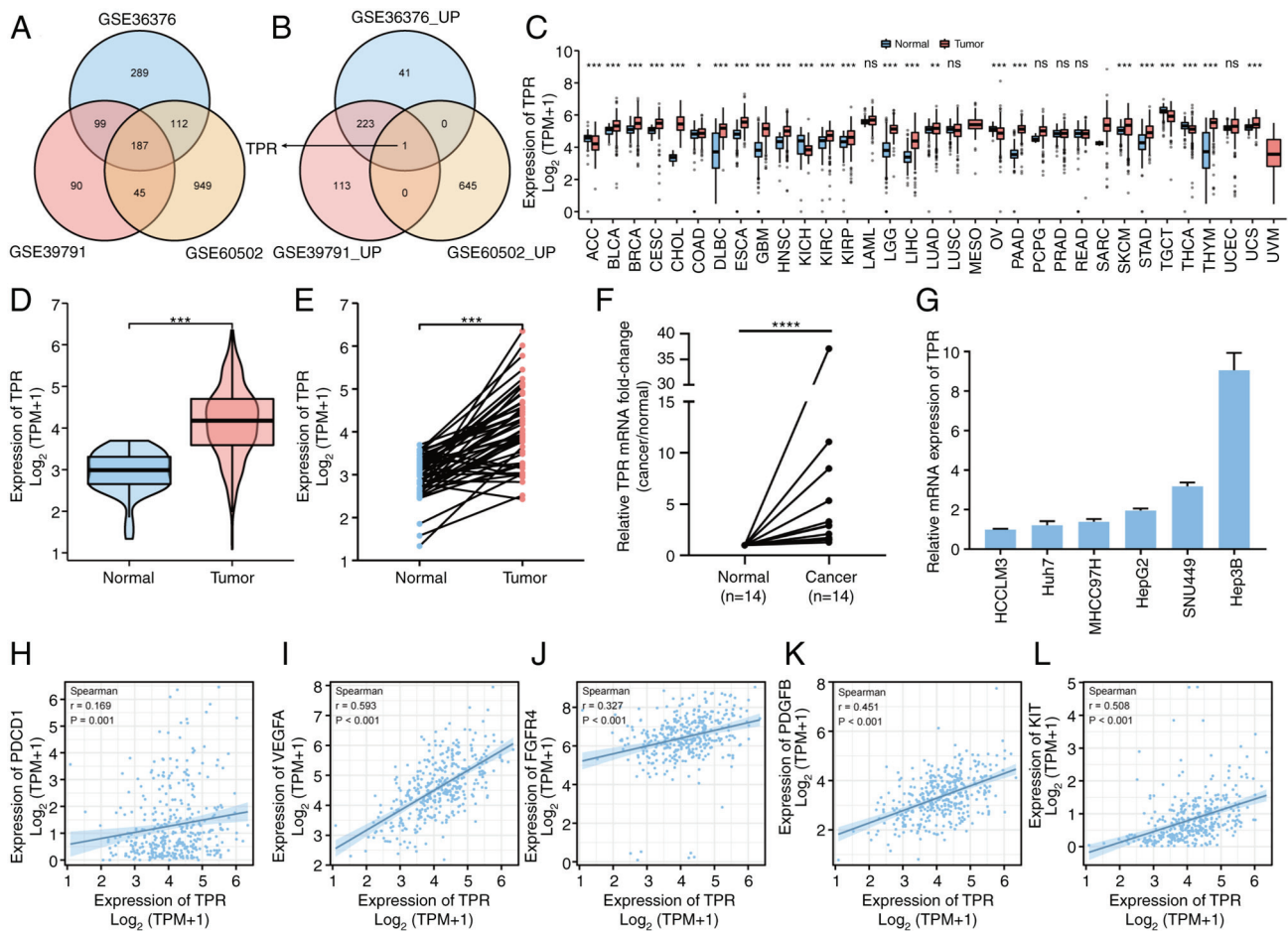


Figure 2. Differential expression map of TPR. (A) Venn diagrams of DEGs and (B) identification of upregulated DEGs in the three gene expression profile datasets. (C) The expression of TPR in tumor and normal tissues of pan-cancer in TCGA and Genotype-Tissue Expression.  $P < 0.05$ ,  $^{**}P < 0.01$ ,  $^{***}P < 0.001$  using the Wilcoxon rank sum test. (D) The expression of TPR in normal and HCC tissues in TCGA database.  $^{***}P < 0.001$  using the Wilcoxon rank sum test. (E) TPR expression in HCC tissues and matched normal tissues from TCGA.  $^{***}P < 0.001$  using the paired t-test. (F) The relative mRNA expression level of TPR in 14 paired HCC and para-cancer tissues were determined by RT-qPCR.  $^{****}P < 0.0001$  using the paired t-test. (G) The transcriptional level of TPR was determined in the indicated cell lines by RT-qPCR. The relative mRNA levels of TPR were normalized to the GAPDH level in the indicated cells. Results are presented as the mean  $\pm$  SD of three independent experiments. Correlation analysis between TPR and (H) PDCD1, (I) VEGFA, (J) FGFR4, (K) PDGFB and (L) KIT at the mRNA level using Spearman's correlation. TPR, translocated promoter region; DEGs, differentially expressed genes; TCGA, The Cancer Genome Atlas; HCC, hepatocellular carcinoma; ns, no significance; RT-qPCR, reverse transcription-quantitative PCR; PDCD1, programmed cell death 1; VEGFA, vascular endothelial growth factor A; FGFR4, fibroblast growth factor receptor 4; PDGFB, platelet derived growth factor subunit B; KIT, KIT proto-oncogene.

DEGs were identified. Notably, TPR was the only upregulated gene and there were no downregulated genes included in the overlap of the three datasets (Figs. 2B and S1). An additional 186 genes were upregulated or downregulated in two datasets and expressed inversely in the other dataset.

The differential expression of TPR in HCC tissues and normal tissues was then explored. Among the expression of TPR in 33 types of tumors assessed from TCGA and GTEx, 24 types expressed significantly more TPR than corresponding normal tissues, 6 types demonstrated no significant difference and 3 types lacked sufficient samples (Fig. 2C). It was further identified that the expression of TPR was significantly higher in 374 tumor cases compared with 50 normal cases ( $P < 0.001$ ; Fig. 2D) and 50 tumor tissues compared with their matched non-tumor tissues from TCGA ( $P < 0.001$ ; Fig. 2E).

Furthermore, RT-qPCR was used to determine TPR expression in 14 pairs of HCC and peritumoral tissues. The findings demonstrated a higher TPR expression in most tumor tissues (Fig. 2F). Subsequently, TPR expression was confirmed

at the mRNA level in liver cancer cell lines (Fig. 2G). Next, the correlation of TPR expression with several types of current HCC therapeutic targets, including programmed cell death protein 1 (PDCD1) (29), vascular endothelial growth factor A (VEGFA) (30), fibroblast growth factor receptor 4 (FGFR4) (31), platelet derived growth factor subunit B (PDGFB) (32) and KIT proto-oncogene (KIT) (33), were investigated (Fig. 2H and L). Notably, there were markedly positive correlations between the expression of TPR and these targets. Collectively, these results demonstrated that TPR was highly expressed in HCC and was associated with several existing therapeutic targets.

**Association between TPR and clinical features.** It was then determined whether the expression of TPR is associated with the clinicopathologic variables of patients with HCC. A total of 374 patients with HCC from TCGA, including 353 males and 121 females, were divided into two categories according to the median expression of TPR: The low expression group



Table I. Expression of TPR associated with clinicopathological characteristics (logistic regression).

Characteristics	Total (N)	Odds ratio (OR)	P-value
T stage (T1 and T2 vs. T3 and T4)	371	0.836 (0.521-1.337)	0.454
N stage (N0 vs. N1)	258	0.366 (0.018-2.905)	0.387
M stage (M0 vs. M1)	272	3.137 (0.396-63.865)	0.325
Pathologic stage (Stage I and Stage II vs. Stage III and Stage IV)	350	0.787 (0.485-1.271)	0.328
Tumor status (Tumor free vs. With tumor)	355	0.754 (0.494-1.148)	0.188
Sex (Male vs. Female)	374	0.764 (0.494-1.179)	0.225
Race (Asian vs. Black or African American and White)	362	1.127 (0.744-1.709)	0.571
Age ( $\leq 60$ vs. $>60$ )	373	1.627 (1.082-2.456)	0.020
Weight ( $\leq 70$ vs. $>70$ )	346	1.461 (0.956-2.237)	0.080
Height ( $<170$ vs. $\geq 170$ )	341	1.189 (0.772-1.834)	0.433
BMI ( $\leq 25$ vs. $>25$ )	337	1.146 (0.747-1.760)	0.532
Residual tumor (R0 vs. R1 and R2)	345	0.473 (0.161-1.249)	0.144
Histologic grade (G1 and G2 vs. G3 and G4)	369	0.592 (0.385-0.906)	0.016
Adjacent hepatic tissue inflammation (None vs. Mild and Severe)	237	0.774 (0.463-1.290)	0.327
AFP (ng/ml) ( $\leq 400$ vs. $>400$ )	280	0.455 (0.254-0.799)	0.007
Albumin (g/dl) ( $<3.5$ vs. $\geq 3.5$ )	300	0.817 (0.473-1.401)	0.465
Prothrombin time ( $\leq 4$ vs. $>4$ )	297	1.077 (0.655-1.774)	0.770
Child-Pugh grade (A vs. B and C)	241	0.550 (0.219-1.329)	0.189
Fibrosis ishak score (0 and 1/2 vs. 3/4 and 5/6)	215	0.668 (0.388-1.146)	0.144
Vascular invasion (No vs. Yes)	318	0.755 (0.474-1.200)	0.235

TPR, translocated promoter region.

and the high expression group, and the clinical and gene expression data of these patients were subsequently analyzed (Table SIII). The results revealed that TPR expression was significantly associated with histologic grade ( $P=0.046$ ), age ( $P=0.042$ ), height ( $P=0.039$ ) and weight ( $P=0.034$ ). An association between TPR expression and other clinicopathologic features was not identified. Based on univariate analyses using logistic regression, it was determined that TPR upregulation in HCC was significantly associated with age ( $P=0.020$ ), histologic grade ( $P=0.016$ ) and AFP level ( $P=0.007$ ) (Table I). As revealed in Fig. 3, TPR expression was significantly associated with AFP ( $P<0.001$ ) and pathological stage (stage I vs. stage III,  $P=0.019$ ), but not sex, tumor status, tumor (T) stage, adjacent hepatic tissue inflammation, vascular invasion, residual tumor or ethnicity. These results indicated that the expression of TPR was associated with several clinicopathologic variables of patients with HCC.

**Clinical value of TPR in patient prognosis.** To evaluate the clinical significance of TPR expression, survival rates between high and low TPR expression levels were compared to determine the association between TPR expression and prognosis. The KM survival analysis demonstrated that there were significant differences in overall survival (OS) relapse-free survival (RFS) and progression-free survival (PFS), between the TPR high and low expression groups ( $P=0.08$ ;  $P=0.033$ ;  $P=0.02$ , respectively) (Fig. 4A-C). The univariate Cox proportional hazards model was then applied, and T stage, metastasis stage, pathological stage and tumor status were identified as potential prognostic factors with

$P<0.05$  for OS. In addition, after multivariate analyses was applied, the expression of TPR was not identified as an independent risk prognostic factor for OS among patients with HCC (Table II). Based on the risk factors identified in the multivariate analysis, nomograms were developed to predict 1-, 3-5-year OS rates for HCC patients (Fig. 4D). Calibration plots were constructed to evaluate the agreement between the predicted and the actual OS using the prognosis model (Fig. 4E). In addition, the area under curve (AUC) of TPR in HCC was 0.885 (95% CI, 0.852-0.918), which suggested high diagnostic accuracy of TPR in HCC (Fig. 4F). These results indicated that TPR was a valuable marker to predict clinical outcomes, along with other clinical features in patients with HCC.

**DEGs, enrichment and interaction networks analysis.** After dividing the patients with HCC into two groups according to their TPR expression, an analysis of the DEGs from the two groups was performed. Based on the analysis, 676 DEGs were identified, among them, 498 genes were upregulated and 169 genes were downregulated (Fig. 5A). The top 10 most downregulated genes were AC107396.1, SAA2, SAA1, HAMP, SAA2-SAA4, CLEC1B, CLEC4G, ACTBP12, AC091729.2 and OR52E8 (data not shown). In addition, the top 10 most upregulated genes (LGALS14, HMGA2, SLC6A14, SLC6A15, MYO3A, FER1L6, BPIFA1, CAPN6, MIR483 and COL2A1) are shown in the gene expression heatmap in Fig. 5B. Notably, HMGA2, which had been demonstrated to be associated with tumor progression (34-36), was the upregulated gene of significant expression according to the volcano plots (Fig. 5A).

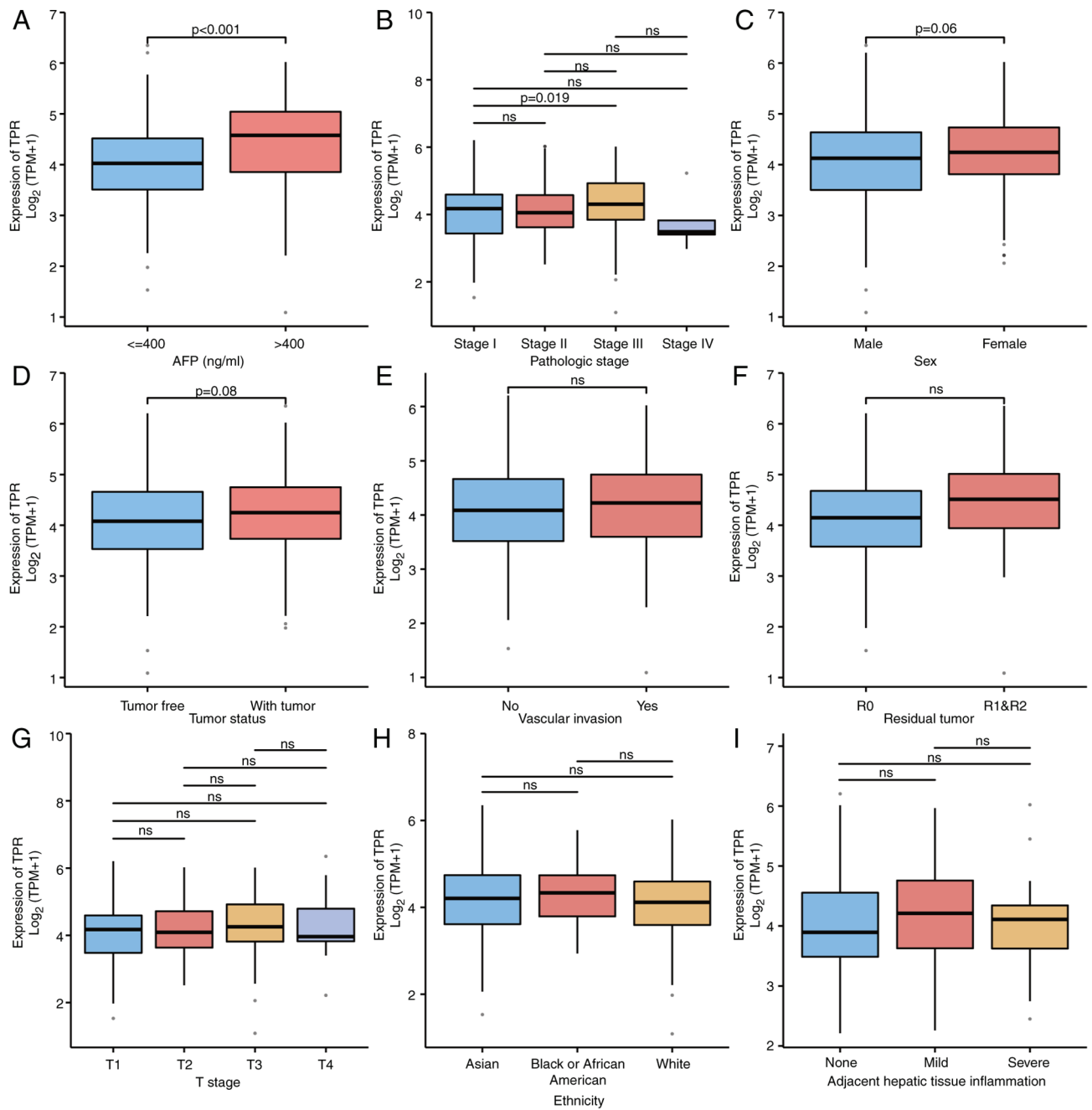


Figure 3. Association of TPR expression and (A) AFP (calculated using the Wilcoxon rank sum test), (B) pathological stage (calculated using the Dunn's test), (C) sex (calculated using the independent samples t-test), (D) tumor status (calculated using the independent samples t-test), (E) vascular invasion (calculated using the independent samples t-test), (F) residual tumor (calculated using the independent samples t-test), (G) T stage (calculated using the Dunn's test), (H) ethnicity (calculated using the Tukey's HSD test) and (I) adjacent hepatic tissue inflammation (calculated using the Tukey's HSD test). TPR, translocated promoter region; AFP, alpha-fetoprotein; T (stage), tumor (stage); ns, no significance.

Therefore, the potential biological functions of TPR in HCC were examined. GO and KEGG analyses were performed using the Metascape database, and the top 20 GO enriched pathways are listed in Fig. 5C. It was notable that the GO enriched items included cell differentiation, which is involved in tumor progression. Moreover, a total of 132 BPs, 34 CCs, 37 MFs and 7 KEGG annotations were associated with TPR co-expressed genes, the results of which are shown by bubbly plots (Fig. 5D-G). Next, GSEA between high and low TPR expression data sets were conducted to explore the signaling pathways differentially activated in HCC. Gene sets with false

discovery rate (FDR) <0.25 and P.adjust <0.05 were considered as significant. The top five most significant signaling pathways enriched in the high TPR expression phenotype according to their normalized enrichment score (NES) are listed in Fig. 5H, including retinoblastoma gene in cancer (NES=2.801; FDR=0.002; P.adjust=0.003), resolution of sister chromatid cohesion (NES=2.703; FDR=0.002; P.adjust=0.003), mesodermal commitment pathway (NES=2.681; FDR=0.002; P.adjust=0.003), mitotic prometaphase (NES=2.658; FDR=0.002; P.adjust=0.003) and endoderm differentiation (NES=2.650; FDR=0.002; P.adjust=0.003).

Table II. Univariate and multivariate analyses of overall survival of patients with hepatocellular carcinoma from The Cancer Genome Atlas (Cox regression).

Characteristics	Total (N)	Univariate analysis		Multivariate analysis	
		Hazard ratio (95% CI)	P-value	Hazard ratio (95% CI)	P-value
T stage	370				
T1 and T2	277	Reference			
T3 and T4	93	2.598 (1.826-3.697)	<b>&lt;0.001</b>	1.769 (0.238-13.138)	0.577
M stage	272				
M0	268	Reference			
M1	4	4.077 (1.281-12.973)	<b>0.017</b>	1.658 (0.384-7.159)	0.498
Pathologic stage	349				
Stage I and Stage II	259	Reference			
Stage III and Stage IV	90	2.504 (1.727-3.631)	<b>&lt;0.001</b>	1.423 (0.193-10.480)	0.729
Tumor status	354				
Tumor-free	202	Reference			
With tumor	152	2.317 (1.590-3.376)	<b>&lt;0.001</b>	1.889 (1.180-3.022)	<b>0.008</b>
Child-Pugh grade	240				
A	218	Reference			
B and C	22	1.643 (0.811-3.330)	0.168		
Vascular invasion	317				
No	208	Reference			
Yes	109	1.344 (0.887-2.035)	0.163		
Race	361				
Asian	159	Reference			
Black or African American & White	202	1.341 (0.926-1.942)	0.121		
TPR	373				
Low	186	Reference			
High	187	1.367 (0.964-1.938)	0.079	1.575 (0.990-2.507)	0.055

Bold indicates P<0.05. TPR, translocated promoter region.

Finally, the gene-gene interaction networks of TPR constructed using GeneMania indicated the top 20 most frequently altered genes (Fig. 5I), while the protein-protein interaction networks generated using STITCH presented the top 10 proteins that most interacted with TPR (Fig. 5J; Table III). These results prompted a further investigation into the potential biological functions of TPR in HCC.

*Correlation between TPR expression and tumor immune infiltration.* GSEA between high and low TPR expression data sets also identified several immune and inflammation-related pathways enriched in the high TPR expression phenotype, including resistin as a regulator of inflammation, immunoregulatory interactions between a lymphoid and a non-lymphoid cell, the inflammatory response pathway, ADORA2B-mediated anti-inflammatory cytokine production, and intestinal immune network for IgA production (data not shown). Given that targeting the tumor microenvironment (TME) is a new treatment strategy for HCC and that immune

Table III. Annotation and respective co-expression scores of proteins that interact with TPR.

Gene symbol	Annotation	Combined score
NUP93	Nucleoporin 93 kDa	0.995
NUP153	Nucleoporin 153 kDa	0.994
NUP98	Nucleoporin 98 kDa	0.994
NXF1	Nuclear RNA export factor 1	0.991
NUP107	Nucleoporin 107 kDa	0.991
U2AF2	U2 small nuclear RNA auxiliary factor 2	0.987
RANBP2	RAN binding protein 2	0.979
NUP205	Nucleoporin 205 kDa	0.978
NUP133	Nucleoporin 133 kDa	0.972

TPR, translocated promoter region.



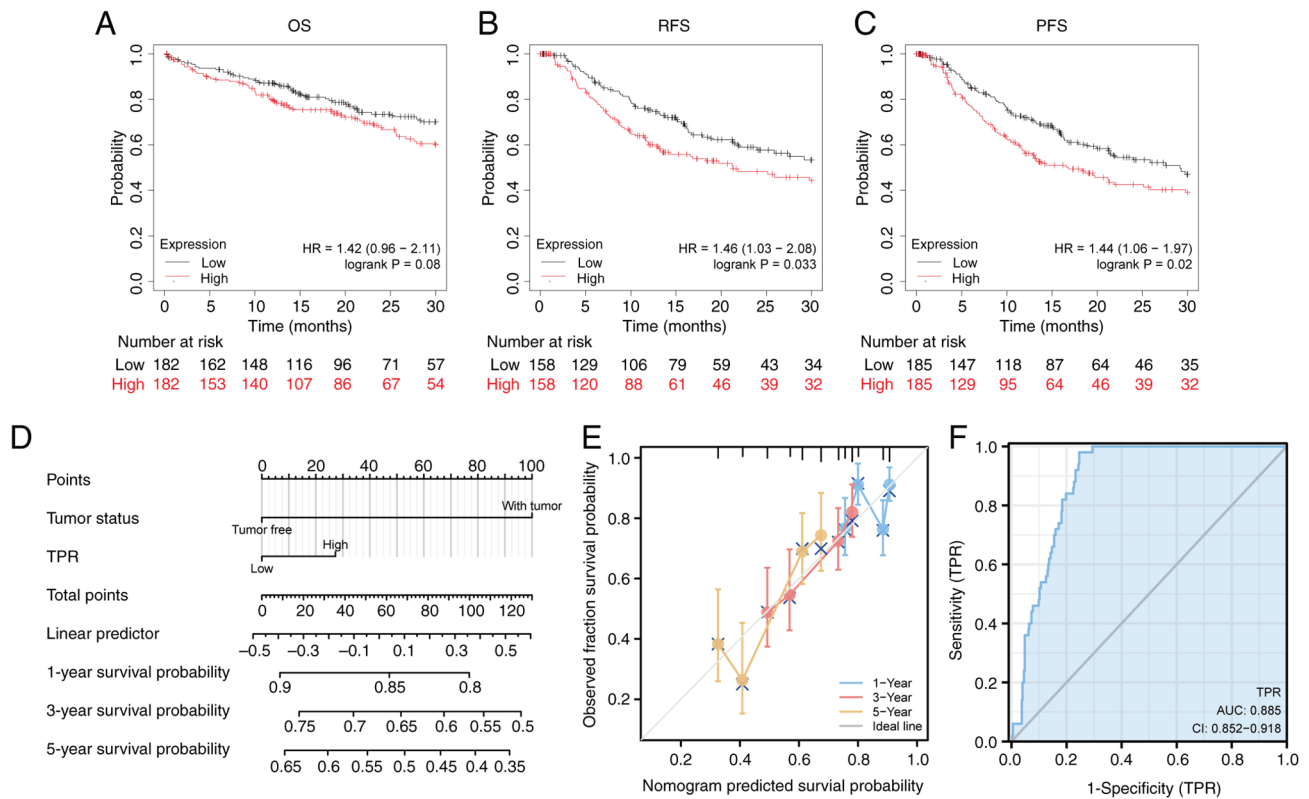


Figure 4. Survival analysis and nomogram of TPR in patients with HCC. The KM survival curves comparing different expression levels of TPR in HCC were constructed using the KM Plotter tool. Survival curves are of (A) OS, (B) RFS and (C) PFS. Probabilities were calculated by the KM method and compared using the log-rank test. (D) Nomogram of predicting the probability of 1-, 3-, 5-year OS rates using Cox regression. (E) Calibration plot of the nomogram. (F) Receiver operating characteristic curve of TPR. TPR, translocated promoter region; HCC, hepatocellular carcinoma; KM, Kaplan-Meier; OS, overall survival; RFS, relapse-free survival; PFS, progression-free survival.

infiltration is a core component of the TME, the correlation between TPR and tumor immune infiltration was determined to further investigate the effect of TPR on the TME. For this purpose, the associations between TPR expression and the number of different tumors infiltrating immune cells in HCC were analyzed utilizing the Xiantao tool. The results indicated that the expression of TPR was negatively correlated with StromalScore ( $\rho = -0.121$ ;  $P = 0.020$ ), ESTIMATEScore ( $\rho = -0.192$ ;  $P < 0.001$ ) and ImmuneScore ( $\rho = -0.218$ ;  $P < 0.001$ ) (Fig. 6A). The correlations between TPR and infiltrating immune cells are shown in Fig. 6B. Elevated expression of TPR was positively correlated with the infiltration of T helper cells ( $\rho = 0.436$ ), Th2 cells ( $\rho = 0.319$ ) and central memory T cell (Tcm) ( $\rho = 0.276$ ), and negatively correlated with cytotoxic cells ( $\rho = 0.421$ ), dendritic cells (DCs;  $\rho = -0.382$ ) and plasmacytoid dendritic cells (pDCs;  $\rho = -0.366$ ) (all  $P < 0.001$ ) (Fig. 6C-H).

A validation study of TPR expression and the diverse immune signature was further conducted to understand the crosstalk between TPR and immune response by TIMER. The gene markers were used to characterize immune cells (Table IV) and functional T cells (Table V). The results revealed that the expression of TPR was significantly associated with most immune and T cell markers after adjusting for tumor purity. As shown in the aforementioned tables, markers of M1 macrophages (IRF5, PTGS2 and NOS2), M2 macrophages (CD163, VSIG4 and MS4A4A), Treg (FOXP3, CCR8 and TGFB1) and exhausted T cells

(HAVCR2, CXCL13 and LAYN) were correlated with TPR in HCC ( $P < 0.001$ ). It was suggested TPR could regulate exhaustion and macrophage polarization in HCC. Next, the association between TPR with immunoinhibitors, such as CSF1R ( $\rho = -0.285$ ;  $P < 0.001$ ), HAVCR2 ( $\rho = -0.275$ ;  $P < 0.001$ ) and TGFB1 ( $\rho = 0.133$ ;  $P = 0.0104$ ) (Fig. 7A), and immunostimulators, including CD40 ( $\rho = -0.296$ ;  $P < 0.001$ ), IL6R ( $\rho = 0.395$ ;  $P < 0.001$ ) and TNFRSF14 ( $\rho = -0.388$ ;  $P < 0.001$ ) (Fig. 7B), were investigated. In addition, the association between the expression of TPR and chemokines, containing CCL5 ( $\rho = 0.377$ ;  $P < 0.001$ ), CCL14 ( $\rho = -0.382$ ;  $P < 0.001$ ) and CXCL2 ( $\rho = -0.324$ ;  $P < 0.001$ ) (Fig. 7C), were explored. Consistently, TPR expression was identified to be significantly associated with chemokine receptors, such as CCR5 ( $\rho = -0.181$ ;  $P < 0.001$ ), CXCR3 ( $\rho = -0.22$ ;  $P < 0.001$ ) and CXCR6 ( $\rho = -0.238$ ;  $P < 0.001$ ) (Fig. 7D). These results demonstrated that TPR was an immunoregulatory factor in HCC and played an integral role in regulating the immune response.

*TPR promotes phosphorylation of AKT and proliferation of HCC cells.* To confirm the bioinformatics results and to verify the effect of TPR on HCC cells, TPR-silenced SNU449 and Hep3B cell lines were constructed (Fig. 8A). It has been reported that regulation of TPR expression affects the phosphorylation activity of the AKT pathway (37). Consistently, the results of WB demonstrated that silencing TPR expression decreased the phosphorylation levels of AKT (Fig. 8B). Next,

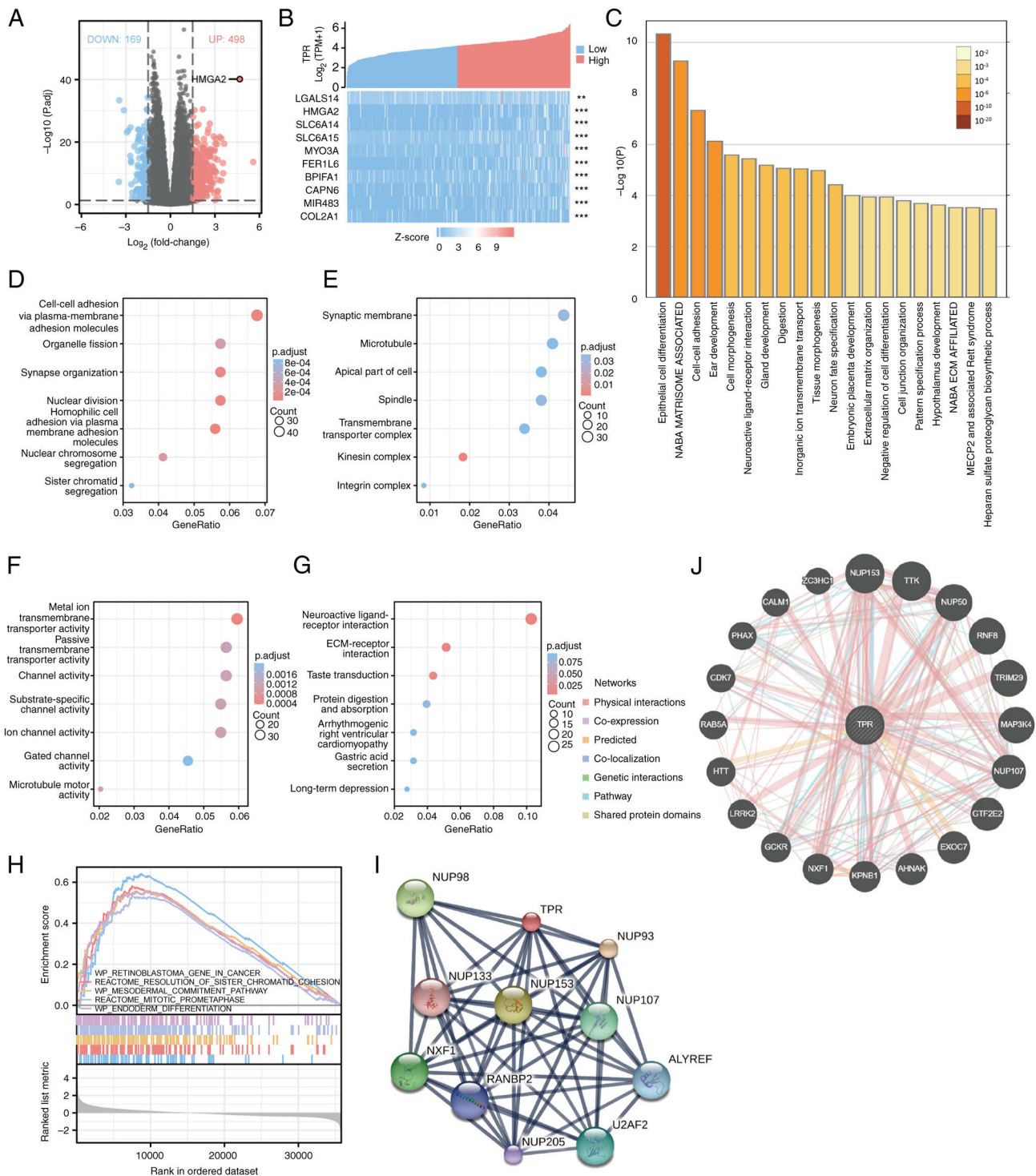


Figure 5. DEG map of HCC in The Cancer Genome Atlas. (A) A volcano map showing the DEGs based on TPR expression. (B) A heat map of the top 10 most upregulated genes generated based on the expression level of TPR. \*\* $P < 0.01$  and \*\*\* $P < 0.001$  using Spearman's correlation. (C) A bar graph of Gene Ontology enriched terms colored by P-value in Metascape. Top seven enrichment terms in (D) biological processes, (E) cellular components and (F) molecular functions and (G) KEGG annotations of HCC. (H) Top five KEGG enrichment pathways in HCC. (I) The gene-gene interaction network of TPR in GeneMania. (J) The protein-protein interaction network of TPR in Search Tool for Interaction Gene/Proteins (minimum required interaction score=0.4). DEG, differentially expressed gene; HCC, hepatocellular carcinoma; TPR, translocated promoter region; Kyoto Encyclopedia of Genes and Genomes.

an MTT assay was conducted to explore the effect of siTPR on the proliferation ability of HCC cells (Fig. 8C). The results demonstrated that after silencing TPR in SNU449 and Hep3B cells, proliferation was significantly inhibited. Therefore, TPR may promote the proliferation of HCC cells through the AKT pathway.

## Discussion

In the present study, the expression level of TPR in HCC and the clinical significance of the gene was comprehensively evaluated by bioinformatics methods. It was demonstrated that high expression of TPR in HCC was associated with

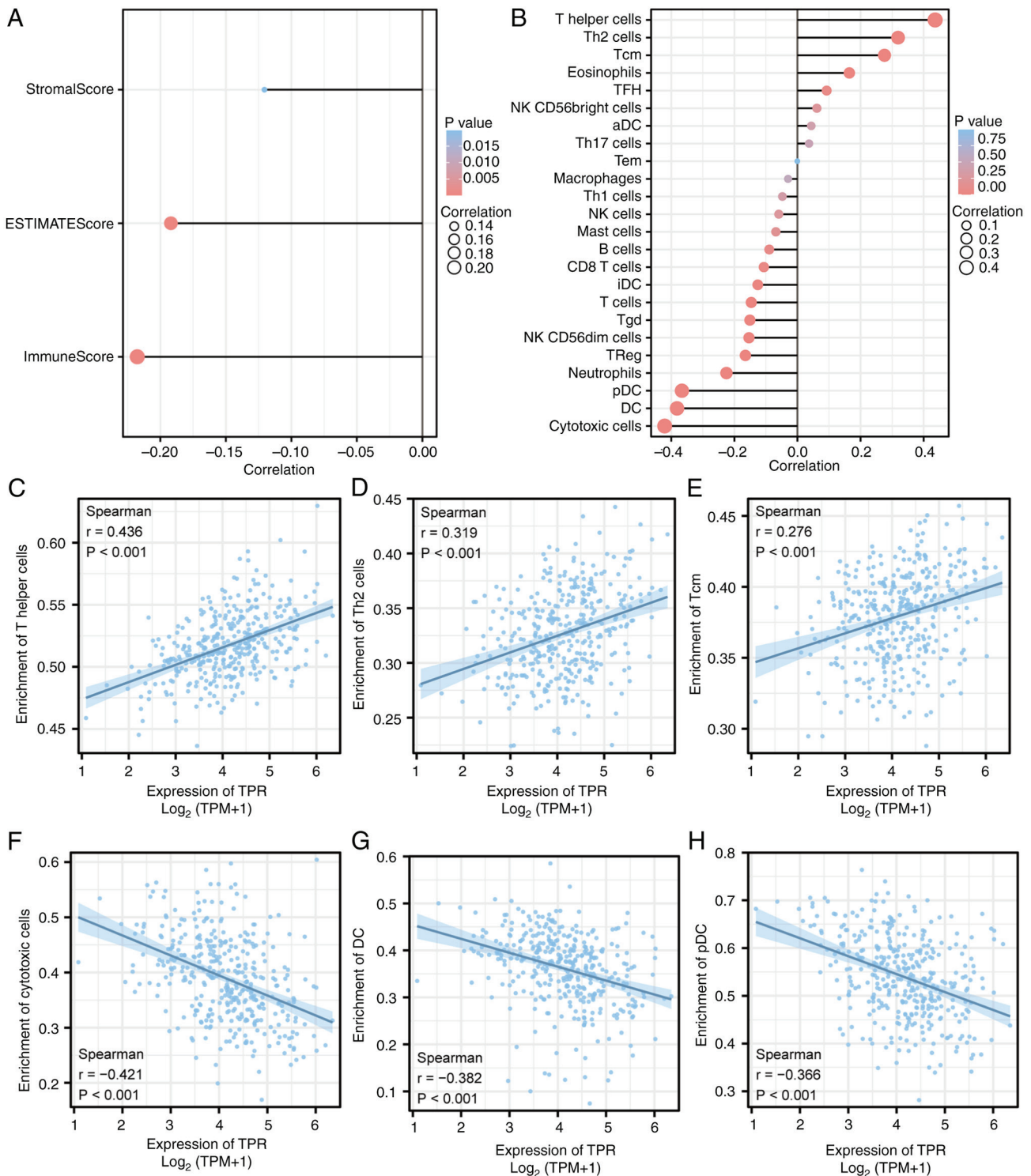


Figure 6. Correlation of TPR expression with immune infiltration in HCC. (A) Correlation of TPR expression with the infiltration levels of StromaScore, ESTIMATEScore and ImmuneScore in HCC using Xiantao tool. (B) Correlation of TPR expression with infiltration levels of different immune cells in HCC using Xiantao tool. Correlation of TPR expression with infiltration levels of (C) T helper cells, (D) Th2 cells, (E) Tcm, (F) cytotoxic cells, (G) DCs and (H) pDCs in HCC. The probabilities were calculated using Spearman's correlation. TPR, translocated promoter region; HCC, hepatocellular carcinoma; Th2, T helper 2; Tcm, central memory T cell; DCs, dendritic cells; pDCs, plasmacytoid dendritic cells.

poor prognosis. In addition, expression of TPR was closely associated with the infiltration of various immune cells, immunomodulators and chemokines. Collectively, these results offer new insights into the roles TPR plays in HCC, which may have a prognostic value for tumor immune infiltration.

Studies have demonstrated that TPR is involved in several types of cancer. For instance, Wei *et al* (19) suggested that the role of a novel TPR-ROS1 fusion was as an oncogenic driver in metastatic non-small cell lung cancer (NSCLC); Choi *et al* (20) reported that the TRP-ALK protein had the potential to transform cells and respond to ALK inhibitor



Table IV. Correlation analysis between TPR and related gene markers of immune cells in TIMER.

Description	Gene markers	HCC			
		None		Purity	
		Cor	P-value	Cor	P-value
B cells	CD19	0.146	0.005	0.211	<0.001
	CD79A	0.077	0.138	0.193	<0.001
T cells	CD3D	0.020	0.703	0.121	0.025
	CD3E	0.078	0.133	0.212	<0.001
CD8+ T cells	CD2	0.056	0.283	0.183	0.001
	CD8A	0.102	0.049	0.207	<0.001
Monocytes	CD8B	-0.014	0.786	0.080	0.141
	CD86	0.197	<0.001	0.345	<0.001
TAM	CSF1R	0.134	0.010	0.272	<0.001
	CCL2	0.111	0.033	0.233	<0.001
M1	CD68	0.168	0.001	0.264	<0.001
	IL10	0.176	0.001	0.287	<0.001
M2	IRF5	0.449	<0.001	0.462	<0.001
	PTGS2	0.267	<0.001	0.420	<0.001
Neutrophils	NOS2	0.222	<0.001	0.236	<0.001
	CD163	0.141	0.007	0.256	<0.001
NK cells	VSIG4	0.091	0.079	0.211	<0.001
	MS4A4A	0.096	0.064	0.219	<0.001
DC cells	CEACAM8	0.025	0.632	0.048	0.371
	ITGAM	0.223	<0.001	0.318	<0.001
	CCR7	0.171	0.001	0.307	<0.001
	KIR2DL1	-0.051	0.331	-0.051	0.349
	KIR2DL3	0.111	0.032	0.156	0.004
	KIR2DL4	0.035	0.496	0.077	0.156
	KIR3DL1	0.053	0.307	0.105	0.052
	KIR3DL2	0.074	0.152	0.140	0.009
	KIR3DL3	0.016	0.762	0.001	0.991
	KIR2DS4	0.043	0.406	0.052	0.334
	HLA-DPB1	0.089	0.087	0.199	<0.001
	HLA-DQB1	0.015	0.772	0.116	0.031
	HLA-DRA	0.153	0.003	0.272	<0.001
	HLA-DPA1	0.155	0.003	0.276	<0.001
	CD1C	0.233	<0.001	0.333	<0.001
	NRP1	0.534	<0.001	0.574	<0.001
	ITGAX	0.276	<0.001	0.403	<0.001

Analyzed using Spearman's correlation. None, correlation without adjustment. Purity, correlation adjusted by purity; Cor,  $\rho$  value of Spearman's correlation; TPR, translocated promoter region; TAM, tumor-associated macrophage.

treatment in NSCLC; Dewi *et al* (21) reported that TPR regulated heat shock transcription factor 1 mRNA trafficking, maintained MTORC1 activity to phosphorylate ULK1, and prevented macroautophagy/autophagy induction in ependymoma. According to these studies, TPR may affect cancer in a significant way and several types of malignancies may be treated by targeting it. However, it is unclear whether TPR has clinical significance in HCC or whether it regulates tumor immunity.

In the present study, according to bioinformatic analyses of high throughput RNA-sequencing data from TCGA, TPR was expressed at a significantly higher level in HCC tissues than in paired normal tissues, indicating that TPR participated in tumorigenesis and progression. Further investigation was conducted into the link between TPR expression and clinicopathological parameters and it was identified that high expression levels of TPR protein were associated with AFP and pathological stage. In addition, a prognostic gene

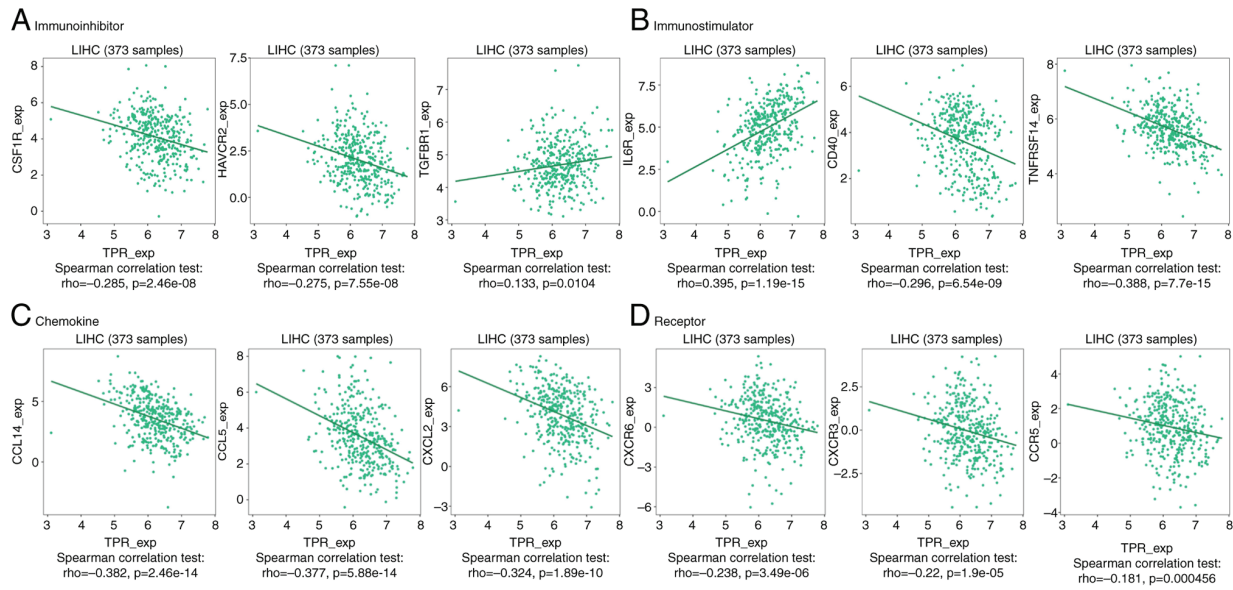


Figure 7. Correlation analysis of TPR expression and (A) immunoinhibitors, (B) immunostimulators, (C) chemokines and (D) chemokine receptors in LIHC using the TISIDB database and Spearman's correlation. TPR, translocated promoter region; LIHC, liver hepatocellular carcinoma; TISIDB, Tumor-Immune System Interactions Database.

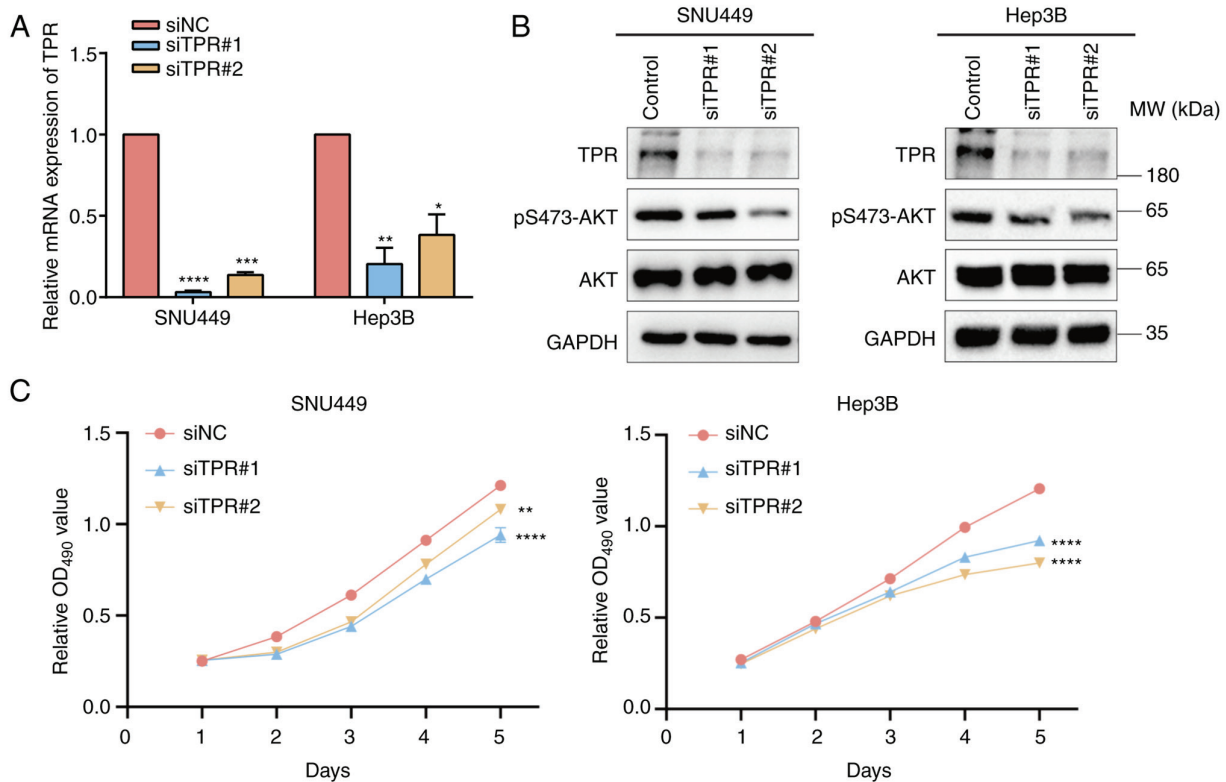


Figure 8. TPR silencing suppresses the phosphorylation of AKT and the proliferation of hepatocellular carcinoma cells. (A) The transcriptional level of TPR was determined in SNU449 and Hep3B cells transfected with siTPR or siNC by reverse transcription-quantitative qPCR. The relative mRNA levels of TPR were normalized to the GAPDH level in the indicated cells. The results are presented as the mean  $\pm$  SD of three independent experiments. \* $P < 0.05$ , \*\* $P < 0.01$ , \*\*\* $P < 0.001$  and \*\*\*\* $P < 0.0001$  using unpaired Student's t-test. (B) The indicated proteins were analyzed by western blotting in SNU449 and Hep3B cells transfected with siTPR or siNC. (C) MTT assays were used to analyze SNU449 and Hep3B cells transfected with siTPR or siNC. \*\* $P < 0.01$ , \*\*\* $P < 0.001$ , \*\*\*\* $P < 0.0001$  using two-way ANOVA with Dunnett's multiple comparison test. TPR, translocated promoter region; si, small interfering; NC, negative control; MTT, 3-(4,5-dimethylthiazol-2-yl)-2,5-diphenyltetrazolium bromide.

signature model based on the KM curve of TPR demonstrated that TPR is valuable for predicting HCC survival, and there was a decrease in OS, RFS and PFS in patients with HCC

with higher TPR expression. Additionally, it was suggested that the expression level of TPR could be used as a diagnostic indicator of HCC with an AUC of 0.885. Taken together, these

Table V. Correlation analysis between TPR and related gene markers of several types of T cells in TIMER.

Description	Gene markers	HCC			
		None		Purity	
		Cor	P-value	Cor	P-value
Th1	TBX21	0.060	0.248	0.156	0.004
	STAT4	0.138	0.008	0.209	<0.001
	STAT1	0.485	<0.001	0.549	<0.001
	TNF	0.240	<0.001	0.354	<0.001
	IFNG	0.078	0.033	0.154	<0.001
Th1-like	HAVCR2	0.172	<0.001	0.321	<0.001
	CXCR3	0.089	0.089	0.185	0.001
	BHLHE40	0.363	<0.001	0.394	<0.001
	CD4	0.157	0.002	0.242	<0.001
Th2	STAT6	0.449	<0.001	0.441	<0.001
	STAT5A	0.318	<0.001	0.385	<0.001
Tregs	FOXP3	0.230	<0.001	0.273	<0.001
	CCR8	0.423	<0.001	0.531	<0.001
	TGFB1	0.282	<0.001	0.398	<0.001
Resting Tregs	FOXP3	0.230	<0.001	0.273	<0.001
	IL2RA	0.225	<0.001	0.347	<0.001
Effector Treg T cells	FOXP3	0.230	<0.001	0.273	<0.001
	CCR8	0.423	<0.001	0.531	<0.001
	TNFRSF9	0.359	<0.001	0.453	<0.001
Effector T cells	CX3CR1	0.409	<0.001	0.457	<0.001
	FGFBP2	-0.019	0.709	-0.009	0.864
	FCGR3A	0.165	0.001	0.267	<0.001
Naive T cells	CCR7	0.171	<0.001	0.307	<0.001
	SELL	0.258	<0.001	0.374	<0.001
Effector memory T cells	DUSP4	0.287	<0.001	0.415	<0.001
	GZMK	-0.017	0.747	0.079	0.144
	GZMA	-0.084	0.106	0.007	0.895
Resident memory T cells	CD69	0.202	<0.001	0.340	<0.001
	CXCR6	0.079	0.131	0.206	<0.001
	MYADM	0.562	<0.001	0.617	<0.001
General memory T cells	CCR7	0.171	<0.001	0.307	<0.001
	SELL	0.258	<0.001	0.374	<0.001
	IL7R	0.328	<0.001	0.465	<0.001
Exhausted T cells	HAVCR2	0.172	<0.001	0.321	<0.001
	LAG3	0.063	0.224	0.115	0.032
	CXCL13	0.115	0.027	0.181	0.001
	LAYN	0.291	<0.001	0.372	<0.001

Analyzed using Spearman's correlation. None, correlation without adjustment; Purity, correlation adjusted by purity; Cor, q value of Spearman's correlation. TPR, translocated promoter region; Th, T helper cell; Treg, regulatory T cell.

results support the hypothesis that TPR could be a prognostic biomarker for HCC.

In addition, valuable insight into the potential key pathways of TPR in HCC were provided in the present study. Metascape revealed that cell differentiation was included in the enriched terms. Consistently, GSEA also demonstrated

that differentiation was enriched in the TPR high expression phenotype. There is evidence that cancer pathogenesis is driven by evading or escaping from terminal differentiation after unlocking the normally restricted capability for phenotypic plasticity (38). Thus, cell plasticity is a promising target for anticancer therapy. The potential connection



between TPR and cell differentiation may be a differentiation therapeutic target in HCC.

A significant correlation between TPR expression and immune infiltration in HCC was also demonstrated in the present study. It was determined that TPR was positively correlated to T helper cells, Th2 cells and Tcm, whereas TPR had an inverse correlation with cytotoxic cells, DC and pDC. Furthermore, TPR was significantly correlated with several immune cell marker sets. For instance, TPR expression was associated with markers of M1 macrophages, IRF5, PTGS2 and NOS2, as well as markers of M2 macrophages, CD163, VSIG4 and MS4A4A. There is an important role for macrophages in proliferation (39), angiogenesis (40), invasion and metastasis (41). According to these results, TPR may regulate polarization of tumor-associated macrophages. In addition, TPR upregulation was also closely associated with Treg markers (FOXP3, CCR8 and TGFB1) and exhausted T cells markers (HAVCR2, LAG3, CXCL13 and LAYN). The main strategy of immunotherapy is to block immune checkpoints (42). Therefore, it is essential to increase the response of tumor cells to immune checkpoint inhibitors and cytokines (43,44). Given that the upregulation of TPR was significantly correlated with immune regulators and chemokines, it is proposed that targeting TPR may improve immunotherapy effectiveness.

Furthermore, in the present study, it was demonstrated that TPR regulated the AKT signaling pathway and tumorigenicity. TPR silencing decreased the phosphorylation levels of AKT and the proliferation of HCC cells. Recently, studies have demonstrated that the AKT pathway regulates cell proliferation and survival (45,46). Consistently, the AKT pathway has been revealed to be hyperactivated in HCC (47). The aforementioned results suggest that acceleration of the malignant behaviors of HCC cells by TPR may be through activating the AKT pathway, although the exact mechanism requires further investigation.

In spite of these results, the present study has some limitations. The results of the present study may be influenced by the fact that most of the data is based on online platforms, which are continuously updated and extended. In addition, the clinical background of these patients is unclear and there may be data collection bias. To avoid confounding differences in the clinical outcomes due to the tumor burdens with those stemming from baseline differences, future research will pay more attention to background information from patients. Secondly, the specific mechanism by which TPR regulates the AKT pathway and other pathways related to TPR in HCC need to be further explored in future studies.

## Acknowledgements

Not applicable.

## Funding

No funding was received.

## Availability of data and materials

The datasets used and/or analyzed during the current study are available from the corresponding author on reasonable request.

## Authors' contributions

TL, WW, XW and MC contributed to the conception and design of the study. TL and WW were responsible for the analysis and interpretation of the data. TL and WW drafted the manuscript. XW and MC revised the manuscript critically for intellectual content. TL, WW, XW and MC confirm the authenticity of all the raw data. All authors read and approved the final version of the manuscript.

## Ethics approval and consent to participate

The present study was conducted according to the ethical guidelines of the 1975 Declaration of Helsinki. The study was approved (approval no. B2022-238-02) by the Research Medical Ethics Committee of Sun Yat-sen University Cancer Center (Guangzhou, China). Informed consent was obtained from all patients.

## Patient consent for publication

All patients signed the informed consent for second use of pathological data and biological specimens.

## Competing interests

The authors declare that they have no competing interests.

## References

- Bray F, Ferlay J, Soerjomataram I, Siegel RL, Torre LA and Jemal A: Global cancer statistics 2018: GLOBOCAN estimates of incidence and mortality worldwide for 36 cancers in 185 countries. *CA Cancer J Clin* 68: 394-424, 2018.
- Sung H, Ferlay J, Siegel RL, Laversanne M, Soerjomataram I, Jemal A and Bray F: Global cancer statistics 2020: GLOBOCAN estimates of incidence and mortality worldwide for 36 cancers in 185 countries. *CA Cancer J Clin* 71: 209-49, 2021.
- European Association for the Study of the Liver. Electronic address: easloffice@easloffice.eu; European Association for the Study of the Liver: EASL clinical practice guidelines: Management of hepatocellular carcinoma. *J Hepatol* 69: 182-236, 2018.
- Kulik L and El-Serag HB: Epidemiology and management of hepatocellular carcinoma. *Gastroenterology* 156: 477-491.e1, 2019.
- Chaiteerakij R, Addissie BD and Roberts LR: Update on biomarkers of hepatocellular carcinoma. *Clin Gastroenterol Hepatol* 13: 237-245, 2015.
- Byrd DA, Sweet DJ, Pante N, Konstantinov KN, Guan T, Sapphire AC, Mitchell PJ, Cooper CS, Aebi U and Gerace L: Tpr, a large coiled coil protein whose amino terminus is involved in activation of oncogenic kinases, is localized to the cytoplasmic surface of the nuclear pore complex. *J Cell Biol* 127: 1515-1526, 1994.
- Cordes VC, Reidenbach S, Rackwitz HR and Franke WW: Identification of protein p270/Tpr as a constitutive component of the nuclear pore complex-attached intranuclear filaments. *J Cell Biol* 136: 515-529, 1997.
- Bangs P, Burke B, Powers C, Craig R, Purohit A and Duxsey S: Functional analysis of Tpr: Identification of nuclear pore complex association and nuclear localization domains and a role in mRNA export. *J Cell Biol* 143: 1801-1812, 1998.
- Cordes VC, Hase ME and Muller L: Molecular segments of protein Tpr that confer nuclear targeting and association with the nuclear pore complex. *Exp Cell Res* 245: 43-56, 1998.
- Hase ME, Kuznetsov NV and Cordes VC: Amino acid substitutions of coiled-coil protein Tpr abrogate anchorage to the nuclear pore complex but not parallel, in-register homodimerization. *Mol Biol Cell* 12: 2433-2452, 2001.

11. Frosst P, Guan T, Subauste C, Hahn K and Gerace L: Tpr is localized within the nuclear basket of the pore complex and has a role in nuclear protein export. *J Cell Biol* 156: 617-630, 2002.
12. Fontoura BM, Dales S, Blobel G and Zhong H: The nucleoporin Nup98 associates with the intranuclear filamentous protein network of TPR. *Proc Natl Acad Sci USA* 98: 3208-3213, 2001.
13. Agarwal S, Yadav SK and Dixit A: Heterologous expression of translocated promoter region protein, Tpr, identified as a transcription factor from *Rattus norvegicus*. *Protein Expr Purif* 77: 112-117, 2011.
14. Krull S, Dörries J, Boysen B, Reidenbach S, Magnusius L, Norder H, Thyberg J and Cordes VC: Protein Tpr is required for establishing nuclear pore-associated zones of heterochromatin exclusion. *EMBO J* 29: 1659-1673, 2010.
15. Aksenova V, Smith A, Lee H, Bhat P, Esnault C, Chen S, Iben J, Kaufhold R, Yau KC, Echeverria C, *et al*: Nucleoporin TPR is an integral component of the TREX-2 mRNA export pathway. *Nat Commun* 11: 4577, 2020.
16. Lee ES, Wolf EJ, Ihn SSJ, Smith HW, Emili A and Palazzo AF: TPR is required for the efficient nuclear export of mRNAs and lncRNAs from short and intron-poor genes. *Nucleic Acids Res* 48: 11645-11663, 2020.
17. Vomastek T, Iwanicki MP, Burack WR, Tiwari D, Kumar D, Parsons JT, Weber MJ and Nandicoori VK: Extracellular signal-regulated kinase 2 (ERK2) phosphorylation sites and docking domain on the nuclear pore complex protein Tpr cooperatively regulate ERK2-Tpr interaction. *Mol Cell Biol* 28: 6954-6966, 2008.
18. Su Y, Pelz C, Huang T, Torkenczy K, Wang X, Cherry A, Daniel CJ, Liang J, Nan X, Dai MS, *et al*: Post-translational modification localizes MYC to the nuclear pore basket to regulate a subset of target genes involved in cellular responses to environmental signals. *Genes Dev* 32: 1398-1419, 2018.
19. Wei S, Hu M, Yang Y, Huang X, Li B, Ding L and Wang P: Case report: Short-term response to first-line crizotinib monotherapy in a metastatic lung adenocarcinoma patient harboring a novel TPR-ROS1 fusion. *Front Oncol* 12: 862008, 2022.
20. Choi YL, Lira ME, Hong M, Kim RN, Choi SJ, Song JY, Pandey K, Mann DL, Stahl JA, Peckham HE, *et al*: A novel fusion of TPR and ALK in lung adenocarcinoma. *J Thorac Oncol* 9: 563-566, 2014.
21. Dewi FRP, Jiapaer S, Kobayashi A, Hazawa M, Ikliptikawati DK, Hartono, Sabit H, Nakada M and Wong RW: Nucleoporin TPR (translocated promoter region, nuclear basket protein) upregulation alters MTOR-HSF1 trails and suppresses autophagy induction in ependymoma. *Autophagy* 17: 1001-1012, 2021.
22. Deland L, Keane S, Bontell TO, Fagman H, Sjögren H, Lind AE, Carén H, Tisell M, Nilsson JA, Ejeskär K, *et al*: Novel TPR::ROS1 fusion gene activates MAPK, PI3K and JAK/STAT signaling in an infant-type pediatric glioma. *Cancer Genomics Proteomics* 19: 711-726, 2022.
23. Moon SW, Mo HY, Choi EJ, Yoo NJ and Lee SH: Cancer-related SRCAP and TPR mutations in colon cancers. *Pathol Res Pract* 217: 153292, 2021.
24. Lim HY, Sohn I, Deng S, Lee J, Jung SH, Mao M, Xu J, Wang K, Shi S, Joh JW, *et al*: Prediction of disease-free survival in hepatocellular carcinoma by gene expression profiling. *Ann Surg Oncol* 20: 3747-3753, 2013.
25. Kim JH, Sohn BH, Lee HS, Kim SB, Yoo JE, Park YY, Jeong W, Lee SS, Park ES, Kaseb A, *et al*: Genomic predictors for recurrence patterns of hepatocellular carcinoma: Model derivation and validation. *PLoS Med* 11: e1001770, 2014.
26. Wang YH, Cheng TY, Chen TY, Chang KM, Chuang VP and Kao KJ: Plasmalemmal vesicle associated protein (PLVAP) as a therapeutic target for treatment of hepatocellular carcinoma. *BMC Cancer* 14: 815, 2014.
27. Knappek KJ, Georges HM, Van Campen H, Bishop JV, Bielefeldt-Ohmann H, Smirnova NP and Hansen TR: Fetal lymphoid organ immune responses to transient and persistent infection with bovine viral diarrhoea virus. *Viruses* 12: 816, 2020.
28. Wang S, Yao X, Ma S, Ping Y, Fan Y, Sun S, He Z, Shi Y, Sun L, Xiao S, *et al*: A single-cell transcriptomic landscape of the lungs of patients with COVID-19. *Nat Cell Biol* 23: 1314-1328, 2021.
29. Zhu Y, Chen M, Xu D, Li TE, Zhang Z, Li JH, Wang XY, Yang X, Lu L, Jia HL, *et al*: The combination of PD-1 blockade with interferon- $\alpha$  has a synergistic effect on hepatocellular carcinoma. *Cell Mol Immunol* 19: 726-737, 2022.
30. Han H, Lin T, Wang Z, Song J, Fang Z, Zhang J, You X, Du Y, Ye J and Zhou G: RNA-binding motif 4 promotes angiogenesis in HCC by selectively activating VEGF-A expression. *Pharmacol Res* 187: 106593, 2022.
31. Yi C, Chen L, Lin Z, Liu L, Shao W, Zhang R, Lin J, Zhang J, Zhu W, Jia H, *et al*: Lenvatinib targets FGF receptor 4 to enhance antitumor immune response of anti-programmed cell death-1 in HCC. *Hepatology* 74: 2544-2560, 2021.
32. Xiao Z, Wang Y and Ding H: XPD suppresses cell proliferation and migration via miR-29a-3p-Mdm2/PDGF-B axis in HCC. *Cell Biosci* 9: 6, 2019.
33. Kalathil SG, Wang K, Hutson A, Iyer R and Thanavala Y: Tivozanib mediated inhibition of c-Kit/SCF signaling on Tregs and MDSCs and reversal of tumor induced immune suppression correlates with survival of HCC patients. *Oncoimmunology* 9: 1824863, 2020.
34. Li DK, Chen XR, Wang LN, Wang JH, Li JK, Zhou ZY, Li X, Cai LB, Zhong SS, Zhang JJ, *et al*: Exosomal HMGA2 protein from EBV-positive NPC cells destroys vascular endothelial barriers and induces endothelial-to-mesenchymal transition to promote metastasis. *Cancer Gene Ther* 29: 1439-1451, 2022.
35. Li Z, Wu X, Li J, Yu S, Ke X, Yan T, Zhu Y, Cheng J and Yang J: HMGA2-Snai2 axis regulates tumorigenicity and stemness of head and neck squamous cell carcinoma. *Exp Cell Res* 418: 113271, 2022.
36. Huang FY, Wong DK, Mak LY, Cheung TT, Seto WK and Yuen MF: Hepatitis B virus X protein promotes hepatocarcinogenesis via the activation of HMGA2/STC2 signaling to counteract oxidative stress-induced cell death. *Carcinogenesis* 43: 671-681, 2022.
37. Che F, Han Y, Fu J, Wang N, Jia Y, Wang K and Ge J: LncRNA MALAT1 induced by hyperglycemia promotes microvascular endothelial cell apoptosis through activation of the miR-7641/TPR axis to exacerbate neurologic damage caused by cerebral small vessel disease. *Ann Transl Med* 9: 1762, 2021.
38. Yuan S, Norgard RJ and Stanger BZ: Cellular plasticity in cancer. *Cancer Discov* 9: 837-851, 2019.
39. Yan K, Wang Y, Lu Y and Yan Z: Coexpressed genes that promote the infiltration of M2 macrophages in melanoma can evaluate the prognosis and immunotherapy outcome. *J Immunol Res* 2021: 6664791, 2021.
40. Pratt HG, Steinberger KJ, Mihalik NE, Ott S, Whalley T, Szomolay B, Boone BA and Eubank TD: Macrophage and neutrophil interactions in the pancreatic tumor microenvironment drive the pathogenesis of pancreatic cancer. *Cancers (Basel)* 14: 194, 2021.
41. Zhang H, Luo YB, Wu W, Zhang L, Wang Z, Dai Z, Feng S, Cao H, Cheng Q and Liu Z: The molecular feature of macrophages in tumor immune microenvironment of glioma patients. *Comput Struct Biotechnol J* 19: 4603-4618, 2021.
42. Pardoll DM: The blockade of immune checkpoints in cancer immunotherapy. *Nat Rev Cancer* 12: 252-264, 2012.
43. Jenkins L, Jungwirth U, Avgustinova A, Iravani M, Mills A, Haider S, Harper J and Isacke CM: Cancer-associated fibroblasts suppress CD8<sup>+</sup> T-cell infiltration and confer resistance to immune-checkpoint blockade. *Cancer Res* 82: 2904-2917, 2022.
44. Asdourian MS, Shah N, Jacoby TV, Semenov YR, Otto T, Thompson LL, Dee EC, Reynolds KL and Chen ST: Development of multiple cutaneous immune-related adverse events among cancer patients after immune checkpoint blockade. *J Am Acad Dermatol* 88: 485-487, 2023.
45. Hua H, Zhang H, Chen J, Wang J, Liu J and Jiang Y: Targeting Akt in cancer for precision therapy. *J Hematol Oncol* 14: 128, 2021.
46. Paskeh MDA, Ghadyani F, Hashemi M, Abbaspour A, Zabolian A, Javanshir S, Razzazan M, Mirzaei S, Entezari M, Goharrizi MASB, *et al*: Biological impact and therapeutic perspective of targeting PI3K/Akt signaling in hepatocellular carcinoma: Promises and challenges. *Pharmacol Res* 187: 106553, 2023.
47. Khemlina G, Ikeda S and Kurzrock R: The biology of Hepatocellular carcinoma: Implications for genomic and immune therapies. *Mol Cancer* 16: 149, 2017.

